analytical chemistry

Article

Cite This: Anal. Chem. 2017, 89, 10850-10857

pubs.acs.org/ac

Biosensing Strategy for Simultaneous and Accurate Quantitative Analysis of Mycotoxins in Food Samples Using Unmodified Graphene Micromotors

Águeda Molinero-Fernández,[‡,§] María Moreno-Guzmán,[‡,§] Miguel Ángel López,[‡] and Alberto Escarpa*[,‡,∥]

[‡]Department of Analytical Chemistry, Physical Chemistry, and Chemical Engineering, University of Alcalá, Carretera Madrid-Barcelona, Km. 33,600, Alcalá de Henares, E-28871 Madrid, Spain

[∥]Chemical Research Institute "Andrés M. del Río" (IQAR), University of Alcalá, Carretera Madrid-Barcelona, Km. 33,600, Alcalá de Henares, E-28871 Madrid, Spain

Supporting Information

ABSTRACT: A high-performance graphene-based micromotor strategy for simultaneous, fast, and reliable assessment of two highly concerning mycotoxins (fumonisin B1 (FB1) and ocratoxin A (OTA)) has successfully been developed. The assay principle is based on the selective recognition from aptamers to the target mycotoxins and further "on-the-move" fluorescence *quenching* of the free aptamer in the outer layer of unmodified reduced graphene (rGO; sensing layer) micromotors. Template-prepared rGO/platinum nanoparticles (PtNPs) tubular micromotors were synthesized rapidly and inexpensively by the direct electrodeposition within the conical pores of a polycarbonate template membrane. The new wash-free approach offers using just 1 μL of sample, a simultaneous and rapid "on-the-fly" detection (2 min) with high sensitivity (limits of detection of 7 and 0.4 ng/mL for OTA and FB1, respectively), and high selectivity. Remarkable accuracy (E_r < 5%) during the mycotoxin determination in certified reference material as well as excellent quantitative recoveries (96−98%) during the analysis of food samples were also obtained. The excellent results obtained allow envisioning an exciting future for the development of novel applications of catalytic micromotors in unexplored fields such as food safety diagnosis.

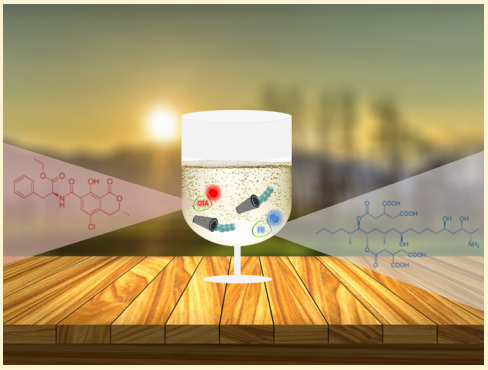

With the purpose of synthesizing tubular microengines[1−3] and Janus particles,[4,5] several approaches including top-down photolithography, e-beam evaporation, and the stress-assisted rolling of functional nanomembranes on polymers has been explored. The complexity and high cost of the conventional fabrication process led to the development of a rapid, easy, and inexpensive template electrodeposition method for preparing bimetallic catalytic nanowires[6,7] and microtubular motors.[8,9] The versatility of template electrosynthesis methods allows exploration of micromotors based on new compositions and structures, with improved catalytic performance and new functionalities essential for diverse new practical applications. Particular attention has been given over the past decade to chemically powered micromotors that exhibit self-propulsion in the presence of hydrogen peroxide fuel.

Efficient bubble propulsion of micromotors was first demonstrated by Schmidt's group.[1,2] Since then, there has been considerable interest in identifying new compositions and structures of micromotors to improve the catalytic performance and characteristics.[10] Indeed, chemically powered micromotors have demonstrated tremendous (bio)sensing opportunities in diverse fields, owing to their attractive "on-the-move" binding, isolation, cargo-towing, and self-mixing capabilities.[11−16]

The utilization of self-propelled micromotors in (bio-) chemical assays has led to a fundamentally new approach where their continuous movement around the sample and the mixing associated effect, due to the generated microbubbles tail, greatly enhances the target−receptor contacts and hence the binding efficiency and sensitivity of the assay. This effect is a particularly important aspect to consider when low sample and reagent volumes are available, where other convection approaches are of lower efficiency to produce adequate interactions.

Nevertheless, despite the great advances in the synthesis and movement of micromotors, they have promoted from their proof of concept into specific applications. Food safety constitutes one relevant example of unexplored areas, which could benefit from these new emerging micromotors-based approaches. Indeed, just one selected work in the agrofood area

Received: June 23, 2017
Accepted: September 10, 2017
Published: September 10, 2017

DOI: 10.1021/acs.analchem.7b02440
Anal. Chem. 2017, 89, 10850−10857

has been identified.[12] In addition, reliable quantitative determination in real samples is still challenging, which is also essential for introduction in the field as new analytical tools.

Carbon nanomaterials met in nanotechnology an enormous source of future diverse applications. One of the carbon nanomaterials that have captured the attention of the scientific community in recent years is graphene, which is a two-dimensional (2D) carbon nanomaterial.[17] Outstanding graphene properties, such as high electrical and thermal conductivities, large surface area, and extraordinary elasticity and mechanical strength,[18−21] make graphene a suitable candidate for advanced micromachine applications.

Graphene has been used for developing tubular micromotors with excellent catalytic performances.[22−24] These pioneering micromotors have exhibited an improved propulsion performance that offers a greatly enhanced catalytic activity and efficient bubble evolution compared with smooth tubular micromotors.[22] Such enhanced catalytic activity along with its improved reactant accessibility and larger surface area enabled a dramatic acceleration of the catalytic reaction. Furthermore, the unique surface properties of graphene have also allowed for the incorporation of different receptors, further allowing toxins detection[25,26] and the capture and removal of nerve agents and heavy metals.[27]

Here we propose a unique analytical application of reduced graphene oxide (rGO)/Pt nanoparticles (PtNPs) microtubular engines as a powerful fluorescent aptamer-based "on−off" strategy for the simultaneous detection of concurrent mycotoxins with high food significance such as ochratoxin A (OTA) and fumonisine B1 (FB1). We hypothesize that continuous movement around the sample and the mixing associated effect, due to the generated microbubbles tail, greatly could enhance the target aptamer−graphene interactions and hence the *quenching* efficiency of the assay.

In the most recent decades, determination of mycotoxins in food commodities has been highly important since they are potent toxins causing negative effects on animals and humans health. Now they are considered the most important chronic dietary risk factor, even more than food additives or pesticide residues.[28] Mycotoxins are identified as inevitable natural secondary metabolites produced by about 200 hundred different filamentous fungi species under different environmental conditions around the world. Due to their negative impact on public health[29−31] low levels of these mycotoxins are permitted in legal requirements of the European Union (0.2 μg/mL for FB and 0.002−0.01 μg/mL for OTA; EC No. 123-2005, EC No.1881-2006, Commission Regulation No. 1126/2007, European Commission, 2007) recommending the development of selective and sensitive approaches. Current methodologies for mycotoxins determination have recently been reviewed and include immunochemical methods and liquid chromatography coupled to tandem mass spectrometry (LC-MS/MS)-based methods.[32] However, the practical application of these methodologies is limited by their nonportability, operational complexity, and difficulties in real-time monitoring.

On the other hand, aptamer-based detection methods have gained great recent interest because of their high selectivity and affinity toward their targets.[33,34] Aptamers are single-stranded oligonucleotides or peptides (typically DNA or RNA) that possess the ability to form defined three-dimensional structure for specific target binding.[35] These aptamers react with their targets (proteins, small molecules, ions, and even cells) with high affinity and specificity, similar to antibodies.[36] Aptamers possess additional advantages such as they are easily synthesized, have a higher specificity and stability, are inexpensive, and can be simply modified with functional groups.[37] For all these advantages, the aptamers are promising alternative recognition elements to antibodies, and they have received tremendous attention in biosensing applications in recent years, including mycotoxin detection.[38−40] In addition, graphene shows excellent aptamer fluorescence quenching ability based on either electron transfer mechanism or energy transfer mechanism.[41] Nucleobase $\pi-\pi$ stacking is responsible for DNA nanostructure adsorption on graphene.[42,43]

Recently, the use of graphene micromotors funcionalized with aptamers has been explored for ricin detection.[26] However, in our view, to expand the field of micromotors for solving real problems in areas of high significance such as food safety diagnosis, analytical validation should be studied. It implies the development of highly stable unmodified micromotors as well as the use of certified reference material (CRM) to demonstrate the traceability and to develop novel approaches with low limits of detection (LODs) in agreement with legal requirements. Here we will illustrate, for the first time, a unique approach using unmodified rGO/PtNPs-based catalytic micromotors for simultaneous, fast, and reliable determination of concurrent high-concern FB and OTA mycotoxins in food samples. The excellent analytical performance in terms of selectivity, sensitivity, accuracy, and precision among the fast detection times and the low sample volumes required for this novel application in food safety diagnosis will be demonstrated in the following sections. Since using micromotors-based (bio-)sensing for food industry is a relatively new field,[44] this work could be contributing to new advances in the area.

EXPERIMENTAL SECTION

Reagents and Samples. The ROX-OTA aptamer, specific for OTA and labeled at the 5′ end with X-rhodamine (ROX), and the FAM-FB aptamer, specific for the FB (FB) and labeled at the 5′ end with fluorescein amidine (FAM), were synthesized by Microsynth (The Swiss DNA Co., Switzerland). The sequence of OTA aptamer was 5′-GGG AGG ACG AAG CGG AAC CGG GTG TGG GTG CCT TGA TCC AGG GAG TCT CAG AAG ACA CGC CCG ACA-3′, and the sequence of FB1 aptamer was 5′-ATA CCA GCT TAT TCA ATT AAT CGC ATT ACC TTA TAC CAG CTT ATT CAA TTA CGT CTG CAC ATA CCA GCT TAT TCA ATT AGA TAG TAA GTG CAA TCT-3′.

Graphene oxide (GO) was purchased from Sigma-Aldrich (2 mg/mL dispersion in H_2O, ref. no. 763705). OTA and FB, hydrogen peroxide, sodium dodecyl sulfate (SDS), H_2SO_4, Na_2SO_4, isopropanol, and ethanol were purchased from Sigma-Aldrich. Hydrogen peroxide solution (1%, v/v) was used as the chemical fuel, and SDS solution (1%, v/v) was used as a surfactant in all propulsion experiments. Aptamers were reconstituted in 10 mM Tris-HCl buffer (pH 7.5; 100 μM) and stored at +4 °C until use. Stock dilutions of OTA and FB (50 μg mL^{-1}) were made in ethanol and acetonitrile: H_2O (50:50, v/v), respectively.

A 100 mM PBS solution (pH 7.5) prepared with Milli-Q water and 0.01% of Tween (PBST) was also used for dilution of ROX−aptamer, FAM−aptamer, and mycotoxins. All chemicals used were of analytical-grade reagents, and deionized

DOI: 10.1021/acs.analchem.7b02440
Anal. Chem. 2017, 89, 10850−10857

water was obtained from a Millipore Milli-Q purification system (18.2 MΩ cm at 25 °C).

Fumonisins maize certified reference material ([FB1] = 2.0 ± 0.4 mg kg^{1-}; [FB2] = 0.5 ± 0.2 mg kg^{1-}; [FB3] = 0.2 ± 0.1 mg kg^{1-}) was purchased from Pribolabs (Singapore). According to the instructions recommended by the supplier, 1 g sample aliquots were extracted with 4 mL of acetonitrile:PBS (50:50, v/v) in cooling refrigeration conditions by a tip sonication (VCX130, Sonics & Materials, Newtown, CT, USA) for 20 min (5 min/cycle) at 117 W. After centrifugation at 4000 rpm during 10 min, the supernatant was separated.

Beer (Guinness Draft, Dublin, Ireland) was previously degasified for 20 min in an ultrasonic bath and spiked with different concentrations of FB. White wine (Cataluña, Spain) was spiked with different concentrations of OTA.

Apparatus. Template electrochemical deposition of micromotors was carried out using an electrochemical station μ-Autolab Type III (Eco Chemie, Utrecht, Holland). Scanning electron microscopy (SEM) images were obtained with a JEOL JSM 6335F instrument, using an acceleration voltage of 22 kV. Energy-dispersive X-ray mapping analysis was performed using an EDX detector attached to a SEM instrument. Raman Dilor XY spectrometer, equipped with two types of detectors: one of type matrix and one photomultiplier, with measurement in sample and by microscope. Equipped with two alternative sources: K^+ Coherent Innova 70C K laser and Ar^+ Coherent Innova 90C laser. An inverted optical microscope (Nikon Eclipse 80i upright microscope), coupled with different objectives (10×, 20×, and 40×), a B2-A fluorescence filter (λ_{ex}, 470 nm; λ_{em}, 520 nm) for FAM, G-2A fluorescence filter (λ_{ex}, 585 nm; λ_{em}, 602 nm) for ROX, and a Hamamatsu digital camera C11440 and NIS Elements AR 3.2 software, were used for capturing images and movies at a rate of 30 frames/s. The speed of the micromotors was tracked using an NIS Elements tracking module. The fluorescence signal produced by the hybridization process between the dye−aptamer and the target toxin was estimated by analyzing the corresponding time lapse images using the Gwyddion software. Aptamer−mycotoxin incubation steps were performed in a thermosaker TS-100C from Biosan (Latvia).

METHODS

Electrosynthesis of Graphene Micromotors. Scheme 1 shows the main two steps involving the electrosynthesis of rGO/PtNPs micromotors. The rGO micromotors were prepared by electrochemical reduction of GO into 5 μm diameter conical pores of a polycarbonate membrane (PC; Catalog No. 7060-2513; Whatman, Maidstone, U.K.).[23] The S4 branched side of the membrane was treated with a sputtered thin gold film to perform as a working electrode. The membrane was assembled in a Teflon plating cell with aluminum foil serving as an electrical contact to the working electrode for the subsequent electrodeposition. GO (0.1 mg/mL) was first dispersed in a solution containing 0.1 M H_2SO_4 and 0.5 M Na_2SO_4 in an ultrasonic bath for 15 min. The electrochemical reduction of GO was carried out using cyclic voltammetry (CV; over +0.3 to −1.5 V vs Ag/AgCl (3 M KCl), at 50 mV s^{-1}, for 10 cycles), using a Pt wire as counter electrode. Subsequently, a platinum layer was plated inside the GO tube. The inner PtNPs layer was deposited by amperometry at −0.4 V for 750 s from an aqueous solution containing 4 mM H_2PtCl_6 in 0.5 M acid boric. The sputtered gold layer was gently hand polished with 1 μm of alumina slurry. After that, the membrane was then dissolved in methylene chloride for 15 min (2 times) to completely release the micromotors. The micromotors were then collected by centrifugation at 7000 rpm for 3 min and washed repeatedly with isopropanol, ethanol, and ultrapure water (18.2 Ω cm), with a 3 min centrifugation following each wash. All micromotors were stored in ultrapure water at room temperature when not in use. The template preparation method is quite simple, taking approximately 120 min for the whole process and giving place to reproducible micromotors.

Scheme 1. Electrosynthesis of rGO/PtNPs Micromotors: (i) Electrodeposition of Outer Sensing Layer (rGO) and Inner Catalytic Layer (PtNPs); (ii) Micromotors Release (Polishing of Sputtered Gold Layer and Dissolving the Polycarbonate Membrane)

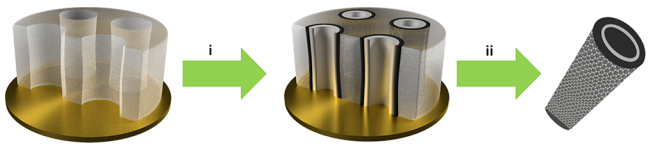

On-the-Fly Mycotoxins Detection. The microscope filters used for OTA and FB fluorescence measurements were a G-2A filter (λ_{ex}, 585 nm; λ_{em}, 602 nm) and B2-A filter (λ_{ex}, 470 nm; λ_{em}, 520 nm), respectively.

A 1 μL aliquot of a mixture of 5 μM of the specific fluorophore-labeled aptamer and the corresponding mycotoxin, previously incubated at 25 °C for their selective recognition during 60 min for OTA and 15 min for FB, were directly positioned onto the microscope slide. Then, graphene micromotors plus 0.5 μL of SDS (1% final concentration) and 1 μL of H_2O_2 (1% final concentration) were added. A continuous monitoring of the quenching of the free aptamer dye, related to the mycotoxin concentration was carried out.

RESULTS AND DISCUSSION

On-the-Fly Strategy for Mycotoxins Detection. The principle assay is based on the selective recognition from aptamers to the highly concerning mycotoxins (FB and OTA) and the binding of free aptamers to the outer layer of graphene micromotors, which led to quenching of the fluorescence of the free-dye-labeled aptamers. Figure 1 illustrates the *on-the-fly* biosensing strategy for mycotoxins detection using unmodified graphene-based micromotors.

In the absence of mycotoxins, the aptamer labeled with fluorophore is adsorbed onto the graphene surfaces through π−π stacking interactions between the ring structures in the nucleotide bases and the hexagonal cells of the carbon material, which drive to a quenching of fluorescence (Figure 1A). Upon the addition of mycotoxins, the high-affinity interaction between mycotoxin and its specific aptamer gives place to the formation of a complex that decreases the exposure of nucleobases to the graphene micromotor, hence allowing its fluorescence. When all the aptamers form the complexes by their binding to the mycotoxins, no fluorescence quenching is observed (fluorescence intensity is the maximum) because no free aptamers are available to be quenched onto the outer surface of graphene micromotors (Figure 1B). Only an excess of free aptamers are adsorbed onto the graphene conducting to a quenching of fluorescence (Figure 1C). In all cases, the quenching of fluorescence is carried out in less than 2 min using

DOI: 10.1021/acs.analchem.7b02440
Anal. Chem. 2017, 89, 10850−10857

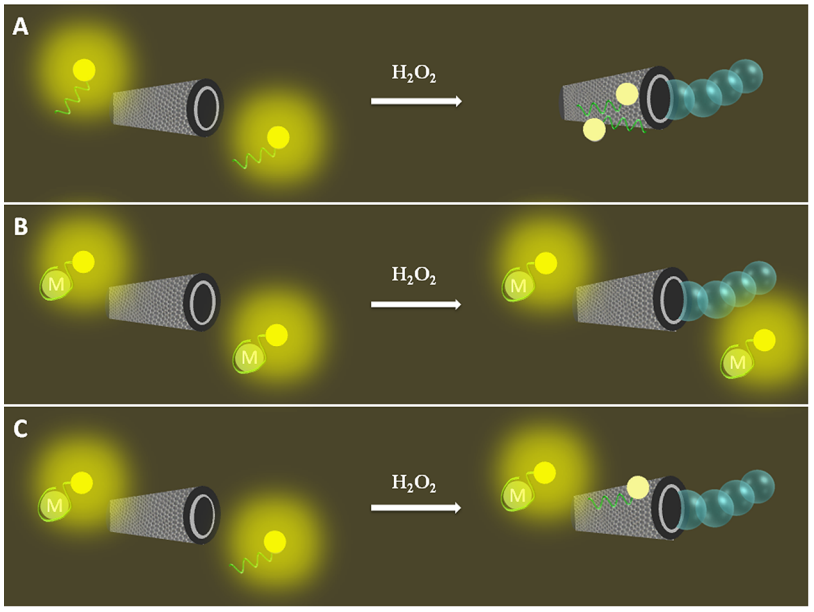

Figure 1. Biosensing strategy for mycotoxins detection using unmodified rGO/PtNPs micromotors: (A) in absence of mycotoxin; (B) in excess of mycotoxin; (C) intermediate mycotoxin concentration.

extremely low sample volumes (1 μL). This strategy is very simple since it used just unmodified graphene-based micromotors, which were synthesized rapidly and inexpensively by the direct electrodeposition without further functionalization.

According to the proposed strategy, Video S1 shows, nicely combined, the following key experiments: (i) at t = 0 min of rGO/PtNPs micromotors navigating, the exhibited fluorescence by the free aptamer (5 μM, in absence of mycotoxin, maximum fluorescence) as well as the exhibited fluorescence by the complex mycotoxin−aptamer (in the presence of 10 μg/mL mycotoxin, maximum fluorescence); (ii) at t = 2 min of rGO/PtNPs micromotors navigating, the total fluorescence *quenching* from the free aptamer by the rGO/PtNPs micromotors (in the absence of mycotoxin), as well as the no quenching of the exhibited fluorescence by the complex mycotoxin−aptamer by the rGO/PtNPs micromotors (in the presence of a 10 μg/mL of mycotoxin) (in the video the mycotoxin selected was OTA and its corresponding aptamer ROX; for more details see the Experimental Section).

Figure 2A shows SEM images of the top and side views of a rGO/PtNPs micromotors. The micromotors are ∼10 μm in length and 5 μm in diameter, reflecting the pore size of the PC membrane. An energy-dispersive X-ray spectroscopy analysis (EDX), with the purpose of demonstrating the successful composition and modification of the rGO/Pt micromotors was carried out, too. These EDX images (Figure 2B) clearly show the presence of carbon and platinum, corresponding to the outer and inner layers, respectively.

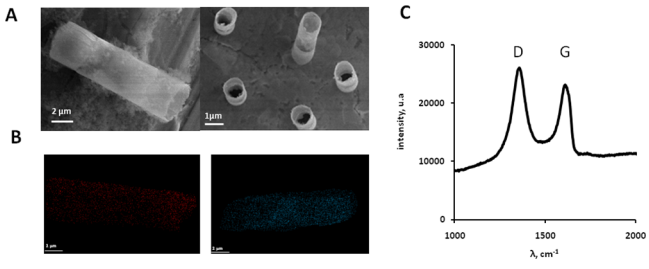

Figure 2. rGO/PtNPs micromotors characterization: (A) SEM images of the rGO/PtNPs micromotors (side views; left and top); (B) EDX analysis of carbon (red) and platinum (blue); (C) Raman spectra of the graphene micromotors.

Raman characterization of rGO/PtNPs micromotors was also performed (Figure 2C). As expected, the Raman spectra of rGO/PtNPs micromotors displayed a well-defined D band at 1347 cm^{-1} and a G band at 1601 cm^{-1}. The D band arises from the out-of-plane vibrational modes and is indicative of the number of sp^3 carbon atoms present, whereas the G band arises from the presence of in-plane sp^2 vibrations. Due to the large two-dimensional surface of graphene, single-stranded DNA can be bound via hydrophobic and $\pi-\pi$ stacking interactions between the ring structures in the nucleobases and the hexagonal cells of graphene.[45,46]

Regarding the biodetection event, different parameters have carefully been optimized. In this sense, using a fixed aptamers concentration (5 μM), the number of micromotors was first studied. Figure 3 shows the influence of the number of motors on the fluorescence quenching. In absence of the mycotoxin, when the number of micromotors increases, fluorescence quenching also increases, 900 motors becoming the optimum value.

Then, the influence of aptamer concentrations on fluorescence quenching were also tested for both mycotoxins becoming 5 μM as optimum concentration. Upon mycotoxin−aptamer binding, the required time for the micromotors to swim into the sample solution and quenching the free fluorophore−aptamers was also studied. Only 2 min was necessary to obtain the maximum fluorescence quenching.

Interestingly, when the static micromotors (as control) are used, only the fluorescence quenching of 50% was obtained, requiring a minimum of 15 min in comparison with the only 2 min required to obtain the maximum flourescence quenching using the dynamic micromotors. Even using an external shaking procedure (with identical sample volumes), no quenching is observed at 2 min, at least 15 min being needed for a quenching

DOI: 10.1021/acs.analchem.7b02440
Anal. Chem. 2017, 89, 10850−10857

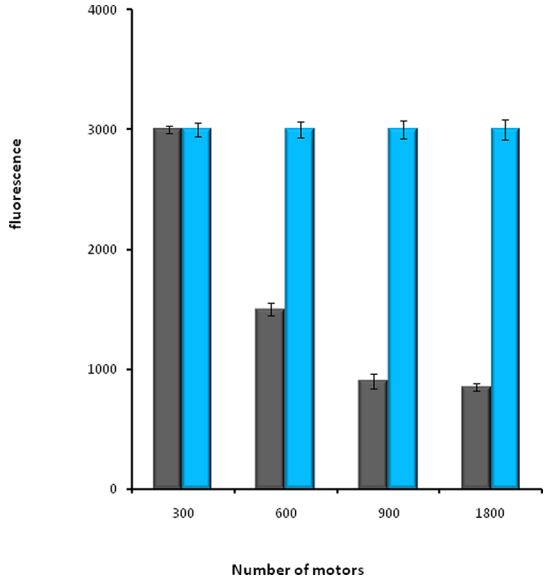

Figure 3. Influence of number of rGO/PtNPs micromotors on fluorescence quenching in presence (blue) and in absence of mycotoxin (gray). The number of motors corresponds with the number of motors contained in each assayed volume (aptamer concentration, 5 μM; FB, 10 μg/mL).

efficiency of about 70%. These results confirm that both movement of the micromotors around the low volume of sample and the mixing effect due to the localized fluid convection and vortex streams associated with the rapid movement of the micromotors together with the generated microbubbles tail greatly improve the graphene-fluorescent/aptamer interaction, and hence the quenching effect. In addition, it is worth mentioning that this extremely short quenching time (just 2 min) contrasts with those published (80 min) using a solution containing a dispersion of graphene and the specific aptamers under normal stirring.[39]

The short assay time, together with the low sample volume needed and the simple procedure, avoiding washing or separation steps, make this method very suitable for the analysis of these mycotoxins in a large number of samples and the potential development of microspots arrays.

Analytical Performance and Quantitative Analysis. Calibration performance was deeply studied since quantitative analysis is rarely explored in the relevant literature in spite of being of paramount importance. Interestingly, Figure 4 clearly exhibits the fluorescence signal variation produced by the nonquenched aptamer−mycotoxin complex vs mycotoxin concentration.

Analytical parameters for both calibration mycotoxins are summarized in Table 1. For both OTA and FB mycotoxins, the assay exhibited an excellent linearity ($r \geq 0.990$) in the concentration ranges studied.

Table 1. Analytical Characteristics for *on-the-Fly* Mycotoxins Determination

analytical characteristic	OTA	FB
linear range (μg/mL)	0.01−10	0.001−10
r	0.990	0.996
sensitivity (mL/μg)	95.7	589.7
LOD (μg/mL)	0.007	0.0004
LOQ (μg/mL)	0.01	0.001
reproducibility (RSD (%), n = 4)	<9	<9

Interestingly, high sensitivity and very good limits of detection were obtained for both mycotoxins in the on-the-fly assay. The LODs obtained (S/N = 3 criteria) agreed with the legal requirements of the European Union (0.2 μg/mL for FB and 0.002−0.01 μg/mL for OTA) since their values were under these permitted levels for both mycotoxins. These values revealed the suitability of this novel strategy for FB and OTA assessment in foods.

Precision was also carefully evaluated at two mycotoxin concentrations (0.01 and 1 μg/mL for the OTA and 0.001 and 1 μg/mL for the FB) yielding excellent values of RSDs ≤ 9% (n = 4 independent micromotor batches).

In order to explore the analytical possibilities for simultaneous mycotoxins detection, selectivity was deeply studied. First, as it is observed in Figure 5 (aptamer selectivity), the incubation of specific aptamer−target mycotoxin (target in

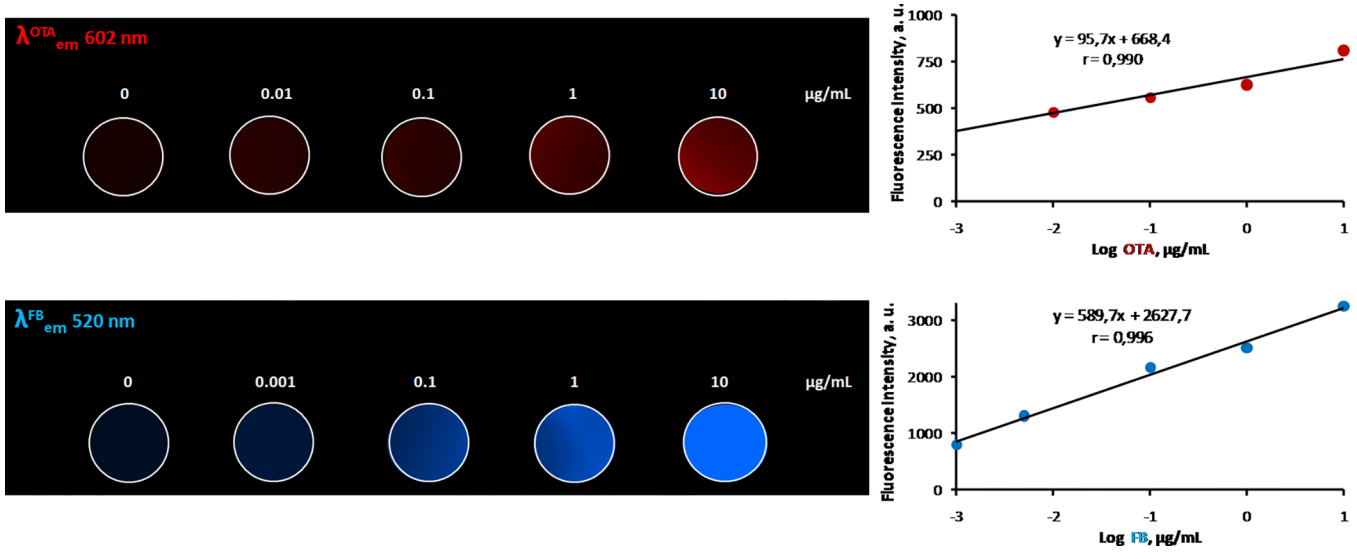

Figure 4. Calibration of OTA and FB using graphene-based micromotors. The red and blue scales are proportional to the emission intensity.

DOI: 10.1021/acs.analchem.7b02440
Anal. Chem. 2017, 89, 10850−10857

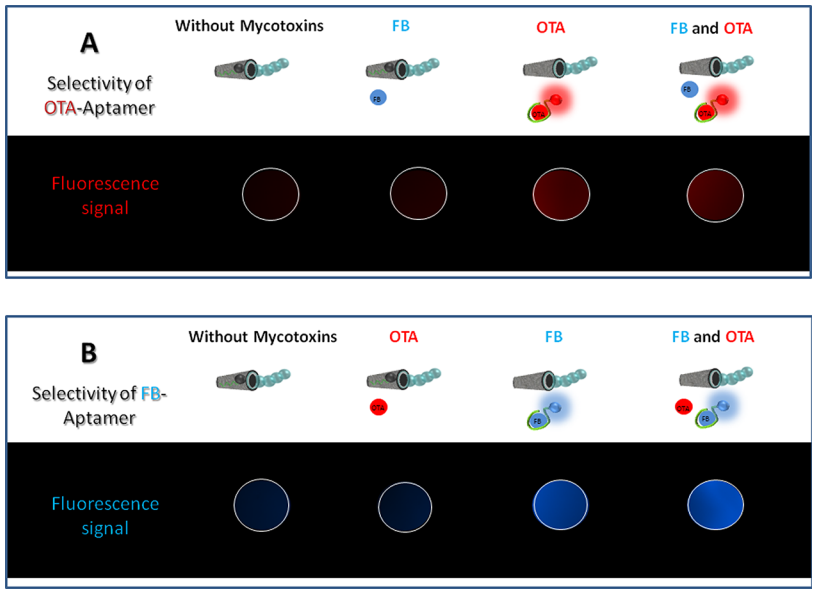

Figure 5. Aptamer selectivity for OTA (A) and FB (B): (A) without mycotoxin, with 1 μg/mL FB, with 1 μg/mL OTA, with 1 μg/mL OTA plus 1 μg/mL FB; (B) without mycotoxin, with 1 μg/mL OTA, with 1 μg/mL FB, with 1 μg/mL OTA plus 1 μg/mL FB.

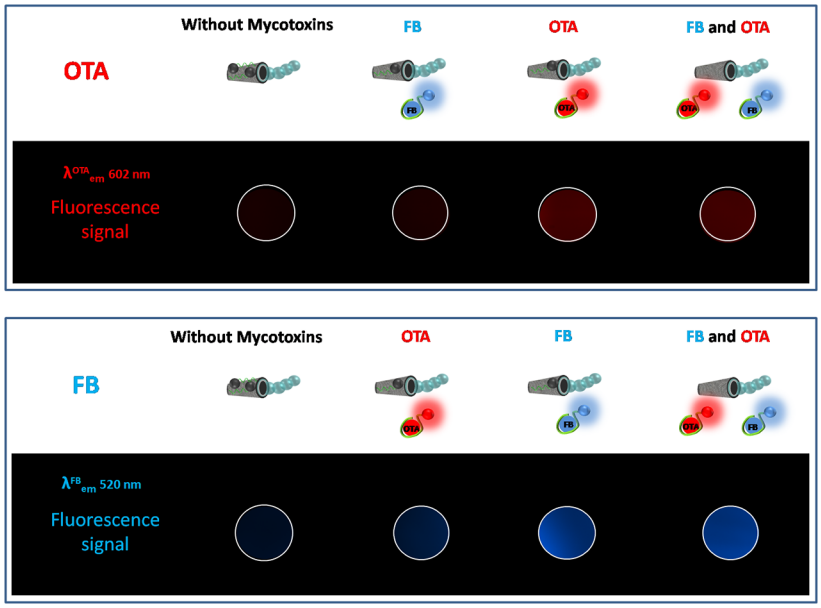

Figure 6. Spectral selectivity: OTA (λ^{OTA}_{em}, 602 nm), without mycotoxin, with 1 μg/mL FB, with 1 μg/mL OTA, with 1 μg/mL FB plus 1 μg/mL OTA; FB (λ^{FB}_{em}, 520 nm), without mycotoxin, with 1 μg/mL OTA, with 1 μg/mL FB, with 1 μg/mL FB plus 1 μg/mL OTA.

A, OTA; target in B, FB) generated the expected fluorescence even in the presence of the nontarget concurrent mycotoxin. However, the sole presence of the nontarget mycotoxin did not avoid the quenching effect of the graphene micromotor.

Further selectivity experiments (spectral selectivity) were also performed where both aptamers were incubated simultaneously with a sample containing both OTA and FB (see Figure 6). As expected, only the target mycotoxin was selectively detected at its optimum λ_{em} (target in A, OTA; target in B, FB) even in the presence of the nontarget mycotoxin.

To evaluate the applicability of developed on-the-fly assay, a certified reference material and food samples were also analyzed.

First, Figure 7 and Video S2 displays the micromotor swimming in different real samples (a–d, PBST buffer, CRM, beer, and wine, respectively) along with 1% H_2O_2 fuel. The rGO/PtNPs micromotors displayed efficient movement in these different media, PBST buffer, CRM, beer, and wine, with speeds of 360 ± 60, 260 ± 50, 320 ± 90, and 280 ± 90 μm s^{-1},

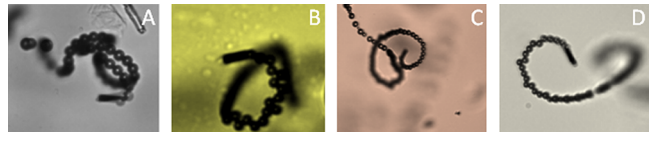

Figure 7. Micromotor swimming in different food samples (from A to D, PBST buffer, CRM, beer, and wine, respectively).

DOI: 10.1021/acs.analchem.7b02440
Anal. Chem. 2017, 89, 10850–10857

Table 2. Analysis of CRM and Food Samples

sample	mycotoxin	reference value (μg/mL)	found value (μg/mL)	E_r (%)	recovery (%)
RM	FB	0.23 ± 0.05	0.24 ± 0.02	4.3	
beer	FB	0.20	0.22 ± 0.02		98 ± 8
wine	OTA	0.20	0.19 ± 0.02		96 ± 6
CRM + OTA (spiked)	FB	0.23	0.23 ± 0.03		100 ± 8
	OTA	1.0	1.1 ± 0.1		110 ± 6

respectively. Interestingly, the fluorescence mycotoxin−aptamer complex in food samples and the quenching effect of the free aptamer by rGO/PtNPs micromotors gave identical values in comparison with those obtained using standards. These results confirmed the efficient micromotors navigation in the food samples.

Finally, quantitative analysis of the food samples was also carried out. Interestingly, the results listed in Table 2 demonstrated an outstanding accuracy when the CRM was analyzed (E_r < 5%) and a good reliability because of the quantitative recoveries (96−98%) obtained during the analysis of food samples. Simultaneous determination of both mycotoxins was also accomplished by the dual aptamer/micromotor-based approach in a fumonisins maize certified reference material containing 0.23 μg/mL FB spiked with 1 μg/mL OTA. In this case, the recoveries obtained were 100 ± 8 and 110 ± 6% (n = 3), respectively.

CONCLUSIONS AND OUTLOOK

In this work, a pioneering agrofood safety diagnosis application using unmodified rGO/PtNPs micromotors for simultaneous quantitative, fast, easily applied, and reliable assessment of OTA and FB mycotoxins is proposed. The new method offers rapid *on-the-fly* (2 min), very sensitive (LODs under legal requirements), and reliable (high selectivity and remarkable accuracy) assessment of concurrent mycotoxins in CRM as well as in complex food samples.

In comparison with the classical aptamer-based biosensors, this novel approach adds valuable advantages such as the extremely low sample volume required, avoids the usual washing steps, and simplifies the overall protocol, while keeping excellent analytical characteristics. These features, make this method very suitable for the analysis of large numbers of samples and the potential development of new envisioned microspot arrays, opening novel avenues for food safety diagnosis.

More importantly, the excellent results obtained allow envisioning an exciting future for the novel applications of micromotors in unexplored fields, entailing a different way to perform analytical operations.

ASSOCIATED CONTENT

Supporting Information

The Supporting Information is available free of charge on the ACS Publications website at DOI: 10.1021/acs.analchem.7b02440.

Video S1 showing on-the-fly strategy for mycotoxins detection (AVI)

Video S2 showing motion of rGO/PtNPs micromotors in food samples (AVI)

AUTHOR INFORMATION

Corresponding Author

*Tel.: +34 91 885 49 95. E-mail: alberto.escarpa@uah.es.

ORCID

Alberto Escarpa: 0000-0002-7302-0948

Author Contributions

§A.M.-F. and M.M.-G. contributed equally to this work.

Notes

The authors declare no competing financial interest.

ACKNOWLEDGMENTS

This work has been financially supported by the NANOAVANSENS program from the Community of Madrid (Grant S2013/MIT-3029), the Spanish Ministry of Economy and Competitiveness Grant CTQ 2014-58643-R from the Spanish Ministerio de Ciencia e Innovación (A.E.). A.M.-F. acknowledges the FPI fellowship from the University of Alcala and FPU fellowship from the Spanish Ministry of Education Culture and Sports. M.M.-G. acknowledges the NANOAVANSENS program from the Community of Madrid (Grant S2013/MIT-3029) for her postdoctoral contract. We thank CAI and CNME of Complutense University of Madrid for the Raman and SEM measurements.

REFERENCES

(1) Mei, Y. F.; Huang, G. S.; Solovev, A. A.; Ureña, E. B.; Mönch, I.; Ding, F.; Reindl, T.; Fu, R. K. Y.; Chu, P. K.; Schmidt, O. G. *Adv. Mater.* **2008**, *20*, 4085−4090.

(2) Solovev, A. A.; Mei, Y. F.; Bermúdez Ureña, E.; Huang, G. S.; Schmidt, O. G. *Small* **2009**, *5*, 1688−1692.

(3) Mei, Y.; Solovev, A. A.; Sanchez, S.; Schmidt, O. G. *Chem. Soc. Rev.* **2011**, *40*, 2109−2119.

(4) Howse, J. R.; Jones, R. A. L.; Ryan, A. J.; Gough, T.; Vafabakhsh, R.; Golestanian, R. *Phys. Rev. Lett.* **2007**, *99*, 048102.

(5) Baraban, L.; Makarov, D.; Streubel, R.; Monch, I.; Grimm, D.; Sanchez, S.; Schmidt, O. G. *ACS Nano* **2012**, *6*, 3383−3389.

(6) Paxton, W. F.; Kistler, K. C.; Olmeda, C. C.; Sen, A.; St. Angelo, S. K.; Cao, Y.; Mallouk, T. E.; Lammert, P. E.; Crespi, V. H. *J. Am. Chem. Soc.* **2004**, *126*, 13424−13431.

(7) Laocharoensuk, R.; Burdick, J.; Wang, J. *ACS Nano* **2008**, *2*, 1069−1075.

(8) Gao, W.; Sattayasamitsathit, S.; Orozco, J.; Wang, J. *J. Am. Chem. Soc.* **2011**, *133*, 11862−11864.

(9) Zhao, G.; Pumera, M. *RSC Adv.* **2013**, *3*, 3963−3966.

(10) Kherzi, B.; Pumera, M. *Nanoscale* **2016**, *8*, 17415−17421.

(11) Wang, J. *Nanomachines: Fundamentals and Applications* ; Wiley-VCH: Weinheim, Germany, 2013.

(12) Guix, M.; Mayorga-Martinez, C. C.; Merkoçi, A. *Chem. Rev.* **2014**, *114*, 6285−6322.

(13) Wang, H.; Pumera, M. *Chem. Rev.* **2015**, *115*, 8704−8735.

(14) Wang, J. *Biosens. Bioelectron.* **2016**, *76*, 234−242.

(15) Wang, J.; Gao, W. *ACS Nano* **2012**, *6*, 5745−5751.

DOI: 10.1021/acs.analchem.7b02440
Anal. Chem. 2017, 89, 10850−10857

(16) Orozco, J.; Campuzano, S.; Kagan, D.; Zhou, M.; Gao, W.; Wang, J. *Anal. Chem.* **2011**, *83*, 7962−7969.
(17) Martín, A.; Escarpa, A. *TrAC, Trends Anal. Chem.* **2014**, *56*, 13−26.
(18) Wang, J. *Faraday Discuss.* **2013**, *164*, 9−18.
(19) Gao, W.; Sattayasamitsathit, S.; Uygun, A.; Pei, A.; Ponedal, A.; Wang, J. *Nanoscale* **2012**, *4*, 2447−2453.
(20) Stankovich, S.; Dikin, D. A.; Dommett, G. H. B.; Kohlhaas, K. M.; Zimney, E. J.; Stach, E. A.; Piner, R. D.; Nguyen, S. T.; Ruoff, R. S. *Nature* **2006**, *442*, 282−286.
(21) Lee, C.; Wei, X.; Kysar, J. W.; Hone, J. *Science* **2008**, *321*, 385−388.
(22) Martin, A.; Jurado-Sanchez, B.; Escarpa, A.; Wang, J. *Small* **2015**, *11*, 3568−3574.
(23) Maria-Hormigos, R.; Jurado-Sanchez, B.; Vazquez, L.; Escarpa, A. *Chem. Mater.* **2016**, *28*, 8962−8970.
(24) Vilela, D.; Parmar, J.; Zeng, Y.; Zhao, Y.; Sanchez, S. *Nano Lett.* **2016**, *16*, 2860−2866.
(25) Cheng, H.; Hu, C.; Zhao, Y.; Qu, L. *NPG Asia Mater.* **2014**, *6*, e113.
(26) Esteban-Fernandez de Ávila, B.; Lopez-Ramirez, M. A.; Báez, D. F.; Jodra, A.; Singh, V. V.; Kaufmann, K.; Wang, J. *ACS Sens.* **2016**, *1*, 217−221.
(27) Shao, Y.; Wang, J.; Engelhard, M.; Wang, C.; Lin, Y. *J. Mater. Chem.* **2010**, *20*, 743−748.
(28) Van Egmond, H. P.; Schothorst, R. C.; Jonker, M. A. *Anal. Bioanal. Chem.* **2007**, *389*, 147−157.
(29) Turner, N. W.; Subrahmanyam, S.; Piletsky, S. A. *Anal. Chim. Acta* **2009**, *632* (2), 168−180.
(30) Jodra, A.; López, M. A.; Escarpa, A. *Biosens. Bioelectron.* **2015**, *64*, 633−638.
(31) Jodra, A.; Hervás, M.; López, M. A.; Escarpa, A. *Sens. Actuators, B* **2015**, *221*, 777−783.
(32) Berthiller, F.; Burdaspal, P. A.; Crews, C.; Iha, M. H.; Krska, R.; Lattanzio, V. M. T.; MacDonald, S.; Malone, R. J.; Maragos, C.; Solfrizzo, M.; Stroka, J.; Whitaker, T. B. *World Mycotoxin J.* **2014**, *7*, 3−33.
(33) Loo, A. H.; Bonanni, A.; Pumera, M. *Nanoscale* **2013**, *5*, 4758−4762.
(34) Song, S.; Wang, L.; Li, J.; Zhao, J.; Fan, C. *TrAC, Trends Anal. Chem.* **2008**, *27*, 108−117.
(35) Famulok, M.; Mayer, G.; Blind, M. *Acc. Chem. Res.* **2000**, *33*, 591−599.
(36) Bunka, D. H. J.; Stockley, P. G. *Nat. Rev. Microbiol.* **2006**, *4*, 588−596.
(37) Lian, Y.; He, F.; Wang, H.; Tong, F. *Biosens. Bioelectron.* **2015**, *65*, 314−319.
(38) Yue, S.; Jie, X.; Wei, L.; Bin, C.; Dou Dou, W.; Yi, Y.; QingXia, L.; JianLin, L.; TieSong, Z. *Anal. Chem.* **2014**, *86*, 11797−11802.
(39) Wu, S.; Duan, N.; Ma, X.; Xia, Y.; Wang, H.; Wang, Z.; Zhang, Q. *Anal. Chem.* **2012**, *84*, 6263−6270.
(40) Wang, C.; Qian, J.; An, K.; Huang, X.; Zhao, L.; Liu, Q.; Hao, N.; Wang, K. *Biosens. Bioelectron.* **2017**, *89*, 802−809.
(41) Zhao, H.; Gao, S.; Liu, M.; Chang, Y.; Fan, X.; Quan, X. *Microchim. Acta* **2013**, *180* (9-10), 829−835.
(42) Morales-Narváez, E.; Merkoçi, A. *Adv. Mater.* **2012**, *24* (25), 3298−3308.
(43) Green, N. S.; Norton, M. L. *Anal. Chim. Acta* **2015**, *853*, 127−142.
(44) Srivastava, S. K.; Schmidt, O. G. *Chem. - Eur. J.* **2016**, *22*, 9072−9076.
(45) Lu, C. H.; Yang, H. H.; Zhu, C. L.; Chen, X.; Chen, G. N. *Angew. Chem., Int. Ed.* **2009**, *48*, 4785−4787.
(46) Pérez-López, B.; Merkoçi, A. *Microchim. Acta* **2012**, *179* (1-2), 1−16.

DOI: 10.1021/acs.analchem.7b02440
Anal. Chem. 2017, 89, 10850−10857